Published for SISSA by Springer

Received: *June 20, 2023*
Revised: *October 30, 2023*
Accepted: *November 5, 2023*
Published: *November 22, 2023*

Inferring astrophysical neutrino sources from the Glashow resonance

JHEP11(2023)164

Guo-yuan Huang, Manfred Lindner and Nele Volmer

Max-Planck-Institut für Kernphysik,
Saupfercheckweg 1, 69117 Heidelberg, Germany
E-mail: guoyuan.huang@mpi-hd.mpg.de, manfred.lindner@mpi-hd.mpg.de, nele.volmer@mpi-hd.mpg.de

Abstract: We infer the ultrahigh energy neutrino source by using the Glashow resonance candidate event recently identified by the IceCube Observatory. For the calculation of the cross section for the Glashow resonance, we incorporate both the atomic Doppler broadening effect and initial state radiation $\overline{\nu}_e e^- \to W^- \gamma$, which correct the original cross section considerably. Using available experimental information, we have set a generic constraint on the $\overline{\nu}_e$ fraction of astrophysical neutrinos, which excludes the μ-damped pγ source around 2σ confidence level under the assumption that neutrino production is dominated by the Δ-resonance. While a weak preference has been found for the pp source, next-generation measurements will be able to distinguish between ideal pp and pγ sources with a high significance assuming an optimistic single power-law neutrino spectrum. The inclusion of multi-pion production at very high energies for the neutrino source can weaken the discrimination power. In this case additional multimessenger information is needed to distinguish between pp and pγ sources.

Keywords: Neutrino Interactions, Cosmic Rays

ArXiv ePrint: 2303.13706

https://doi.org/10.1007/JHEP11(2023)164

Contents

JHEP11(2023)164

1 Introduction

The IceCube Observatory has successfully established the observation of ultrahigh energy (UHE) neutrino flux below a few PeV energies [1–8]. However, it remains a mystery as to where those neutrinos come from. One of the most popular mechanisms rests on accelerated cosmic rays colliding with ambient targets around the source [9–14]. There is a variety of source models for UHE neutrinos [15–18] which can usually be classified into the pγ and pp types depending on whether the target particle is a photon or a proton.

For both pγ and pp sources, after traveling an astronomical distance the fluxes of three neutrino flavors strongly mix with each other due to neutrino oscillations, which ends up with a nearly democratic flavor composition $\phi^{\oplus}_{\nu_e} + \phi^{\oplus}_{\overline{\nu}_e} : \phi^{\oplus}_{\nu_\mu} + \phi^{\oplus}_{\overline{\nu}_\mu} : \phi^{\oplus}_{\nu_\tau} + \phi^{\oplus}_{\overline{\nu}_\tau} \approx 1 : 1 : 1$ at Earth.[1] It is unlikely to disentangle those two sources by traditional flavor ratio measurements [19–35]. The difference between those two sources lies in the composition of neutrinos and antineutrinos. For the pγ neutrino source, cosmic rays collide with photons to produce charged pions (mostly π^+ below a certain energy threshold) followed by the decays $\pi^+ \to \mu^+\nu_\mu$ and $\mu^+ \to e^+\overline{\nu}_\mu\nu_e$, which results in more neutrino flux than antineutrino flux, i.e., $\phi^{\rm S}_\nu : \phi^{\rm S}_{\overline{\nu}} = 2 : 1$. In comparison, the pp source will give rise to nearly equal fractions of π^+ and π^-, which leads to $\phi^{\rm S}_\nu : \phi^{\rm S}_{\overline{\nu}} = 1 : 1$.

The key to distinguishing those two sources is by measuring the $\overline{\nu}_e$ fraction $f_{\overline{\nu}_e} \equiv \phi_{\overline{\nu}_e}/(\phi_{\overline{\nu}_e} + \phi_{\nu_e})$, thanks to the Standard Model process $\overline{\nu}_e e^- \to W^- \to X$ predicted by S.L. Glashow [36]. Due to the resonance enhancement, the cross section of $\overline{\nu}_e e^-$ scattering around $E_\nu \approx 6.3\,\text{PeV}$ is larger than that of the deep inelastic scattering (DIS) by more than two orders of magnitude. This promises us an excellent channel to differentiate between the ideal pp (with $f^{\oplus}_{\overline{\nu}_e} \approx 0.5$) and p$\gamma$ (with $f^{\oplus}_{\overline{\nu}_e} \approx 0.23$) sources, as continuously anticipated

---

[1] Throughout this work, we use the superscript '$\oplus$' to denote the quantity at Earth and 'S' to denote that at source.

in previous works [37–53]. It is worthwhile to emphasize that the above argument holds only for ideal pp and pγ cases. Other possible neutrino sources such as neutron and charm decays can give rise to a $\overline{\nu}_e$ fraction different from the typical pion decays. Moreover, if the multi-pion channel in the pγ scattering dominates the neutrino production when the collision energy is very high, more multimessenger information about the source in addition to the ν_e fraction is necessary to disentangle the source degeneracy. In practice, the overall diffuse neutrino flux might be contributed by different types of sources, and the $\overline{\nu}_e$ fraction $f^{\oplus}_{\overline{\nu}_e}$ can take any reasonable values in between. In this regard, we shall first treat the $\overline{\nu}_e$ fraction as a free parameter to be determined by the experimental probes regardless of the model assumptions. The experimental information about this parameter can then be used for theoretical interpretations under specific source assumptions.

Excitingly, with its unprecedented detection volume, the IceCube Observatory has collected one candidate event with an energy deposition $E_{\rm dep} = 6.05 \pm 0.72\,{\rm PeV}$ in the sample of partially contained events [1]. The probability that this event stems from the Glashow resonance (GR) is high, around 99% by using the best-fit neutrino flux taken from ref. [54]. In this work, a timely quantitative assessment is carried out to infer the $\overline{\nu}_e$ fraction by taking $f^{\oplus}_{\overline{\nu}_e}$ as a free parameter and to explain the level that we can differentiate between pγ and pp sources. We have included both the radiation of initial photons [55–57] and the Doppler broadening effect [58] while calculating the GR events. Using the updated cross section, we investigate both the results for the current GR candidate in IceCube as well as the prospects of next-generation experiments.

2 A full treatment of Glashow resonance

As more and more UHE neutrino data have been accumulated, it becomes increasingly important to take into account the subleading effects for the theoretical evaluation of the GR. There are mainly two effects that should be emphasized: (i) the initial state radiation (ISR) [55, 56]; (ii) the Doppler broadening effect [58]. At the leading level, the cross section for the process $\overline{\nu}_e e^- \to W^- \to X$ reads [1]

$$\sigma^{(0)}(s) = 24\pi \Gamma^2_W {\rm Br}_{W^- \to \overline{\nu}_e e^-} \frac{s/M^2_W}{(s - M^2_W)^2 + \Gamma^2_W M^2_W} \,, \tag{2.1}$$

where $M_W \approx 80.433\,{\rm GeV}$ is the mass of the W boson, $\Gamma_W \approx 2.09\,{\rm GeV}$ is the total decay width and ${\rm Br}_{W^- \to \overline{\nu}_e e^-} \approx 10.7\%$ is the branching ratio of the channel $W^- \to \overline{\nu}_e e^-$. The ISR and the Doppler broadening effect are found to considerably modify the above picture and should be included for completion.

Let us start with the ISR. This effect becomes increasingly notable when the center-of-mass (COM) energy is much higher than the mass of the initial charged lepton, for which the collinear emission of photons is significant. For instance, in the Large Electron-Positron Collider (LEP), the ISR should be taken into account when analyzing the Z boson peak [59]. For UHE neutrino telescopes like IceCube, the ISR cross section near the GR will receive a large enhancement factor of $\ln(M_W/m_e) \approx 12$ on top of the fine structure constant α.

The ISR can be consistently included by using the structure function approach in analogy with the DIS off hadrons. The modified cross section will be [56]

$$\sigma(E_\nu) = \int \mathrm{d}x\, \Gamma_{e/e}(x, Q^2)\sigma^{(0)}(x, Q^2, E_\nu)\,, \tag{2.2}$$

where Q represents the energy scale, x is the longitudinal momentum fraction of the electron after the photon radiation, $\sigma^{(0)}$ is the cross section without the initial-state photon, and $\Gamma_{e/e}$ is the structure function of the electron. We take the structure function from ref. [60] which includes soft photons resummed to all orders and hard photons up to $\mathcal{O}(\alpha^3)$.

The second effect of interest is the Doppler broadening due to the motion of atomic electrons [58]. The velocity of atomic electrons β is typically of the order $\mathcal{O}(\alpha\, c)$. A simple estimation shows that this velocity will shift the COM energy square from $s = 2E_\nu m_e$ to $2E_\nu m_e(1 - \beta\cos\theta)$, where θ is the angle between the electron velocity and the incoming neutrino in the laboratory frame. This broadens the COM energy by around 0.6 GeV in comparison to the W decay width $\Gamma_W =$ 2.09 GeV. Non-relativistic electrons in the atom have the four-momentum $(m_e + |\boldsymbol{k}|^2/(2m_e), \boldsymbol{k})$, where $|\boldsymbol{k}| \approx m_e\beta$. By integrating over the electron wave function, one can arrive at the total cross section [58]

$$\sigma(E_\nu) = \frac{1}{4\pi}\int \mathrm{d}\phi \int \mathrm{d}\beta F(\beta) \int \mathrm{d}x' \sigma^{(0)}[E_\nu(1 - \beta x')]\,, \tag{2.3}$$

where ϕ represents the azimuth angle, $F(\beta)$ is the velocity distribution of electrons and $x' = \cos(\theta)$. Since the calculation framework was already outlined in ref. [58], we give more details about the updated calculation in appendix A.

Those two effects can be combined, and their joint result is shown as the red curve in figure 1 for the H_2O target, along with the cross sections without (solid black curve) or modified by only one (blue and orange curves) of those effects. In comparison, the charged-current (CC) and neutral-current (NC) interactions are depicted as dashed and dotted black curves, respectively. Some remarks on the results are given below.

- The ISR will reduce the peak at the resonance energy $E_\nu \approx 6.3$ PeV by almost 20%. Furthermore, the cross section above the resonance energy is enhanced by a factor of more than two. This is due to the radiative return phenomenon, for which the photon in the process $\overline{\nu}_e e^- \to W^-\gamma$ carries away some energy such that the W production will be made on shell even if $\sqrt{s} > M_W$.

- The Doppler broadening effect for the H_2O target is small compared to the ISR in the logarithmic scale. To see the detailed impact we also show the result in a flat scale as figure 4. The resonance peak is reduced slightly, while the width is broadened due to the motion of atomic electrons.

- The combined result of the ISR and the Doppler broadening is obtained with a convolution, which reduces the peak by around 30%. However, we should note that those effects will be partly smeared by the finite energy resolution of the IceCube detector. We have checked that the eventual effect can decrease the events within the energy window near the GR by almost 10%.

JHEP11(2023)164

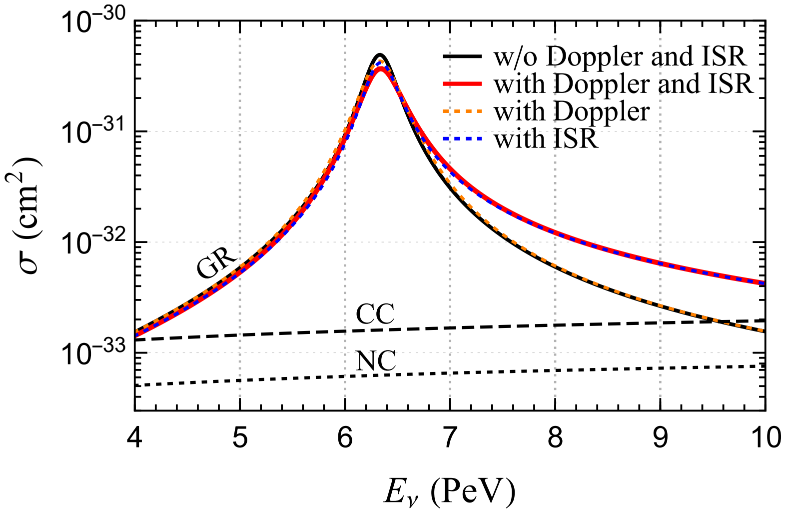

Figure 1. Cross section for the Glashow resonance process $\overline{\nu}_e + e^- \to W^- \to X$ with and without the initial state radiation and Doppler broadening effect. The black curve shows the cross section without initial state radiation and Doppler broadening, the blue dotted one includes initial state radiation and the orange dotted one includes Doppler broadening. The red curve is the cross section with both Doppler broadening and initial state radiation effects, and the tabulated result of this curve is given in our supplementary material. Both the broadening and the radiative return are visible. For the Glashow resonance curves we averaged over the electrons in H_2O for the target.

With the full GR cross section, we are able to calculate the event rate in IceCube and compare it to both experimental data available now and those from future experiments.

3 Analysis framework

In order to constrain the $\overline{\nu}_e$ fraction in the total diffuse neutrino flux, we calculate the likelihood by fitting models with different values of $f_{\overline{\nu}_e} = \phi_{\overline{\nu}_e}/(\phi_{\overline{\nu}_e} + \phi_{\nu_e})$ to the available IceCube data. The reason why we use $f_{\overline{\nu}_e}$ to measure the $\overline{\nu}_e$ fraction is that it almost solely determines the spectrum of single cascade event topology at PeV energies in the IceCube detector.

The observed GR candidate in IceCube belongs to the PeV energy partially contained events (PEPEs), in comparison to the high energy starting events (HESEs) where the shower is fully contained inside the fiducial volume. Even though the PEPE effective volume is nearly twice the volume of HESE at PeV energies only one event with an energy deposition $E_{\text{dep}} = 6.05 \pm 0.72$ PeV has been observed within the energy window 4 PeV $< E_{\text{dep}} <$ 10 PeV. For HESE three PeV events have been collected [61], nicknamed Bert, Ernie and Big Bird. However, all of them have energies below 3 PeV, which are most likely contributed by the DIS. Even though the GR has not significantly arisen in the HESE sample, HESE is useful to fix the normalization and shape of UHE neutrino flux which are crucial for our extraction of the $\overline{\nu}_e$ fraction.

In ref. [6], the IceCube collaboration has analyzed the overall UHE neutrino flux with HESEs collected over 7.5 years, assuming a flavor ratio $\phi^{\oplus}_{\nu_e} + \phi^{\oplus}_{\overline{\nu}_e} : \phi^{\oplus}_{\nu_\mu} + \phi^{\oplus}_{\overline{\nu}_\mu} : \phi^{\oplus}_{\nu_\tau} + \phi^{\oplus}_{\overline{\nu}_\tau} =$

$1:1:1$. During our analysis we will use the HESE results including uncertainties from ref. [6] to set the spectrum of neutrino flux and use PEPE to extract the $\overline{\nu}_e$ fraction $f^{\oplus}_{\overline{\nu}_e}$. Note that a more thorough analysis would assume a completely free flavor ratio. However, on the one hand, the latest IceCube HESE fit available has fixed the flavor ratio [6]. On the other hand, ideal pp and pγ astrophysical models reasonably prefer such a democratic ratio after neutrino oscillations over an astronomical distance.

For demonstration, we choose two benchmark flux models in our analysis: (i) the unbroken single power-law model; (ii) the single power-law model with an exponential energy cutoff. The former one reads

$$\frac{\mathrm{d}\Phi_{6\nu}}{\mathrm{d}E_\nu} = \Phi_0 \left(\frac{E_\nu}{100\,\mathrm{TeV}}\right)^{-\gamma} 10^{-18}\,\mathrm{GeV}^{-1}\,\mathrm{cm}^{-2}\,\mathrm{s}^{-1}\,\mathrm{sr}^{-1}\,, \tag{3.1}$$

which represents models consistent with the Fermi acceleration mechanism and extends to infinite energies. In practice, the reachable energy of astrophysical accelerators always features a cutoff due to the Hillas criterion [62]. For the cutoff model, the flux in eq. (3.1) will be multiplied by a suppression factor $\exp\left(-E_\nu/E_{\mathrm{cutoff}}\right)$. To confine the flux parameters, we construct a likelihood based on the results in ref. [6]:

$$-2\ln\mathcal{L}_{6\nu} = \frac{(\Phi_0-\Phi_0^{\mathrm{bf}})^2}{\sigma(\Phi_0)^2} + \frac{(\gamma-\gamma^{\mathrm{bf}})^2}{\sigma(\gamma)^2}\,, \tag{3.2}$$

with the best-fit values $\Phi_0^{\mathrm{bf}} = 6.37$ and $\gamma^{\mathrm{bf}} = 2.87$, as well as the 1σ errors $\sigma(\Phi_0) = 1.54$ and $\sigma(\gamma) = 0.2$. For the cutoff model we further derive the likelihood for E_{cutoff} from figure VI.9 of ref. [6] where the test-statistic has been marginalized. Note that in this case we have ignored possible correlations among Φ_0, γ and E_{cutoff}, which are not provided. Nevertheless, such a choice will be more conservative because less information is utilized in our analysis.

After the prior knowledge of $\{\Phi_0, \gamma(, E_{\mathrm{cutoff}})\}$ has been established by HESE, we continue with fitting $f^{\oplus}_{\overline{\nu}_e}$ to PEPE. The task is to calculate the likelihood $\mathcal{L}_{\overline{\nu}_e}(f^{\oplus}_{\overline{\nu}_e})$ with the GR candidate we have. The joint likelihood can then be obtained with $\mathcal{L}_{\mathrm{tot}} = \mathcal{L}_{6\nu} \times \mathcal{L}_{\overline{\nu}_e}$ for the parameter set $\Theta \equiv \{\Phi_0, \gamma(, E_{\mathrm{cutoff}}), f^{\oplus}_{\overline{\nu}_e}\}$. In the frame of extended likelihood analysis of unbinned data [63], the likelihood is calculated with

$$\mathcal{L}_{\overline{\nu}_e} = \prod_{i=1}^{n} \left[\mu_{\mathrm{DIS}} P_{\mathrm{DIS}}(\#i|\Theta) + \mu_{\mathrm{GR}} P_{\mathrm{GR}}(\#i|\Theta)\right] \times \frac{1}{n!} \mathrm{e}^{-(\mu_{\mathrm{DIS}}+\mu_{\mathrm{GR}})}\,, \tag{3.3}$$

where μ_{DIS} and μ_{GR} are the expected event numbers within the energy window $E_{\mathrm{dep}} \in [4, 10]$ PeV for the DIS and the GR, respectively, and $\#i$ represents in general all possible GR candidates. Moreover, $P_{\mathrm{DIS/GR}}(\#i|\Theta)$ is the normalized probability to have an event at $\#i$'s energy for the given model parameter set Θ. Since there is only one GR candidate so far we have $n = 1$ in eq. (3.3). The event numbers can be obtained by integrating the flux and cross sections with the detector configuration.

4 Main results

With the framework above, we can compute the total likelihood $\mathcal{L}_{\mathrm{tot}}$ as a function of the parameter set $\{\Phi_0, \gamma(, E_{\mathrm{cutoff}}), f^{\oplus}_{\overline{\nu}_e}\}$. The likelihood can then be used for either frequentist or Bayesian interpretations. For the frequentist interpretation, we obtain the likelihood maximum $\mathcal{L}^{\rm max}_{\rm tot}(f^{\oplus}_{\overline{\nu}_e})$ by marginalizing over the other parameters. For the Bayesian interpretation, we need to derive the posterior distribution of $f^{\oplus}_{\overline{\nu}_e}$ by integrating over the likelihood and priors. We choose flat priors on Φ_0, γ, $f^{\oplus}_{\overline{\nu}_e}$ and $\ln E_{\rm cutoff}$ for illustration.

Our main results are given in figure 2, which shows the likelihood function (in blue) or posterior distribution (in brown) of the $\overline{\nu}_e$ fraction $f^{\oplus}_{\overline{\nu}_e}$ inferred from the IceCube 4.6-year data. Uncertainties from neutrino flux parameters have been systematically included and marginalized when we constrain $f^{\oplus}_{\overline{\nu}_e}$. The upper and lower panels stand for the assumptions of an unbroken single power-law flux model and a single power-law model with a varying exponential energy cutoff, respectively [6]. For blue curves, the horizontal lines with $-2\ln\mathcal{L} = 1$ and 4 roughly set the 1σ and 2σ confidence levels. For brown regions, the 1σ and 2σ credible intervals have been covered from dark to light colors.

We find that for all cases, the μ-damped pγ source with $f^{\oplus}_{\overline{\nu}_e} \approx 0$ (single-pion production via the $\mathit{\Delta}$-resonance for the ideal scenario) is excluded by around 2σ level. The current IceCube 4.6-year data weakly favor the pp source but are not able to exclude the ideal pγ source considerably (only at 1σ or so); see the dashed vertical lines. While interpreting the above results, one must keep in mind that neutrinos may not only be produced by the ideal $\mathit{\Delta}$-resonance of the pγ scattering, but also by other possible effects that can dominate at high energies [64, 65], such as multi-pion production, higher resonances, and the direct (t-channel) production of pions. Note that the above considerations do not affect our model-independent results of $f^{\oplus}_{\overline{\nu}_e}$ extracted from experimental data. For those cases, the theoretically expected value of $f^{\oplus}_{\overline{\nu}_e}$ for the $p\gamma$ source will shift towards larger values. The actual magnitude of the deviation depends on the details of the π^+ and π^- mixture at the source. For demonstration, we assume that the single-pion and multi-pion channels have the same production rate at the source and draw the expected value $f^{\oplus}_{\overline{\nu}_e} \approx 0.36$ as the dotted vertical lines in figure 2. If the multi-pion channel contributes more, this vertical line should move even further to the right. On the other hand, for the pp source the multi-pion contribution does not change the expected value of $f^{\oplus}_{\overline{\nu}_e}$.

Last but not least we should emphasize that the GR event can also constrain the possible energy cutoff $E_{\rm cutoff}$ in the neutrino spectrum. The original best-fit value of $E_{\rm cutoff}$ without GR is around 5 PeV in ref. [6], with a 2σ lower boundary at 0.5 PeV. The presence of the GR candidate event will push the 2σ lower boundary to 2.2 PeV, as illustrated in figure 3.

5 Outlook

Using the recent GR candidate event identified by IceCube, we have performed an analysis to infer the $\overline{\nu}_e$ content in UHE astrophysical neutrinos. We treat the $\overline{\nu}_e$ fraction as a model-independent free parameter and have set a generic constraint on it by including the uncertainties in the UHE neutrino flux. From the candidate event measured so far, we find a weak preference for the pp source under the ideal assumption. The situation will be greatly improved by the upcoming next-generation neutrino telescopes. If the neutrino production in the pγ source is dominated by other channels at higher energies such as

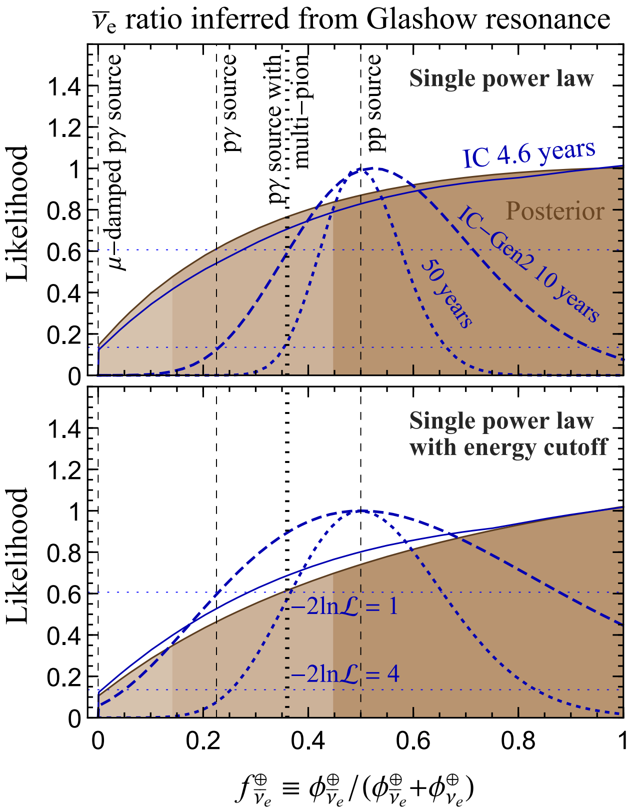

Figure 2. The likelihood (in blue) or posterior (in brown) of the $\overline{\nu}_e$ fraction $f^{\oplus}_{\overline{\nu}_e}$ inferred from the Glashow resonance event in IceCube with 4.6 years of data taking. The upper panel assumes a single power-law flux model with central values and uncertainties from ref. [6], while the lower one has incorporated an exponential cutoff $E_{\rm cutoff}$ in the neutrino spectrum. The expected $\overline{\nu}_e$ fractions of three representative ultrahigh energy neutrino source models, including the ideal pp ($f^{\oplus}_{\overline{\nu}_e} \approx 0.5$), the ideal p$\gamma$ ($f^{\oplus}_{\overline{\nu}_e} \approx 0.23$) and the ideal μ-damped pγ ($f^{\oplus}_{\overline{\nu}_e} \approx 0$) sources, are indicated by the dashed vertical lines. When the pγ collision energy at the source is very high, we may expect deviations from those ideal source models. By assuming an equal mixture of single-pion and multi-pion production at the source, we find the expected value $f^{\oplus}_{\overline{\nu}_e} \approx 0.36$ at Earth, shown as the dotted vertical lines. If multi-pion production is more dominant than this assumption, the expected $f^{\oplus}_{\overline{\nu}_e}$ should move to even larger values. The sensitivity of the future IceCube-Gen2 project with an effective exposure of ten (fifty) years is shown as the dashed (dotted) blue curves, assuming that the pp source is dominant with $\Phi_0 = 6.37$, $\gamma = 2.7$ and $E_{\rm cutoff} = 5\,{\rm PeV}$.

multi-pion production, we would need additional information from the multi-wavelength observations of the source to distinguish between pp and pγ sources.

In the future, there are many projects such as IceCube-Gen2 [66, 67], Baikal-GVD [68], KM3NeT [69], P-ONE [70], TAMBO [71], TRIDENT [72] and so on, which will provide very valuable sensitivities to PeV astrophysical neutrinos [73–76]. We take IceCube-Gen2 for demonstration by rescaling the current IceCube target mass by ten times, and perform a count analysis in the energy window of $[4, 10]\,{\rm PeV}$. The sensitivity for ten (fifty) years of effective exposure is shown as the dashed (dotted) curves in figure 2. Because the flux

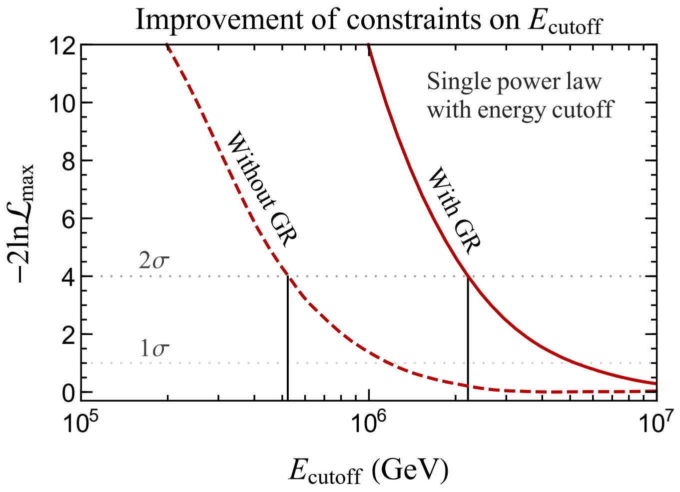

Figure 3. The log-likelihood of the energy cutoff $E_{\rm cutoff}$. The dashed curve is taken from figure VI.9 of ref. [6], while the solid curve is derived from the Glashow resonance candidate event by marginalizing over the other model parameters.

parameters $\{\Phi_0, \gamma(, E_{\rm cutoff})\}$ can be very precisely determined in the future [67], we choose a reasonably optimistic spectrum as $\Phi_0 = 6.37$, $\gamma = 2.7$ and $E_{\rm cutoff} = 5\,{\rm PeV}$ in making the forecast; see figure 16 of ref. [67] for example. It is worth noting that the tau neutrino telescope TAMBO can be sensitive to the Glashow resonance event by searching for the tau-induced showers from W decays. Unfortunately, with a dedicated simulation close to the TAMBO setup, we find that the event number is too small, e.g., only two events with an optimistic flux and ten years of exposure, compared to the DIS background of $\mathcal{O}(100)$. We will elaborate on the related analysis in a future work.

Assuming the pp type as the true source, i.e., $f_{\overline{\nu}_e}^{\oplus} = 0.5$, we expect eleven GR events in IceCube-Gen2 with ten years of exposure for the optimistic single power-law model. If we take an exponential cutoff $E_{\rm cutoff} = 5\,{\rm PeV}$ in the spectrum, the event expectation would be reduced to three. The expected number of events is still diverse due to low statistics of events at PeV energies. For the single power-law model, IceCube-Gen2 with ten years of exposure can already differentiate ideal pp from pγ sources with a 2σ confidence level. However, if there is an exponential cutoff at 5 PeV, an effective exposure of fifty years would be required to reach the 2σ level. Those results can also be applied to other telescopes by adjusting the effective exposure. By measuring the spectrum precisely in the future, one may go beyond the assumptions of single power-law flux model (with cutoff) and take the spectrum with a general energy dependence.

The hybrid cascade and early muon reconstruction in IceCube can already greatly improve the angular resolution of the GR shower. In case of the increased statistics, GR events detected in future experiments can also be used to produce a map of the sky and identify associated PeVatrons [77–79]. Our main point is that knowledge about neutrino sources will be significantly improved by those upcoming facilities with large statistics, which also guarantees a robust frontier for possible new physics studies [80–89].

A Details of the Doppler broadening effect

We follow the procedure outlined in ref. [58] to include the Doppler broadening effect of atomic electrons. By integrating over angular variables in eq. (2.3), we arrive at

$$\sigma(E_\nu) = \frac{6\pi\Gamma_W^2 \mathrm{Br}_{W^-\to\bar{\nu}_e e^-}}{M_W m_e E_\nu} \int d\beta \frac{F(\beta)}{\beta} \left\{ \frac{1}{2M_W} \left[\ln(y_h^2+1) - \ln(y_l^2+1)\right] \right. \\ \left. + \frac{1}{\Gamma_W} \left[\arctan(y_h) - \arctan(y_l)\right] \right\} \tag{A.1}$$

where

$$y_h = \frac{2m_e E_\nu (1+\beta) + m_e^2 - M_W^2}{\Gamma_W M_W} \quad \text{and} \quad y_l = \frac{2m_e E_\nu (1-\beta) + m_e^2 - M_W^2}{\Gamma_W M_W} . \tag{A.2}$$

Now the problem is attributed to the integration over the averaged electron velocity distribution $F(\beta)$. In terms of the wave function of an electron with quantum numbers n and l, the distribution reads

$$f_{n\,l}(\beta) = m_e \int \mathrm{d}\Omega_k k^2 |\Psi_{n\,l}(k)|^2 \quad \text{with} \quad \Psi_{n\,l}(\mathbf{k}) \propto Y_{l\,m}^*(\Omega_k) \int_0^\infty \mathrm{d}r\, r^{n+1} e^{-\mu r} j_l(kr) , \tag{A.3}$$

where $k = m_e\beta$ and $\mu_{n\,l} = \xi_{n\,l}/a_0$. Here, a_0 denotes the Bohr radius, $\xi_{n\,l} = Z_{\mathrm{eff}}/n = (Z - \sigma_{n\,l})/n$, and $\sigma_{n\,l}$ accounts for the screening of the nuclear charge by the other electrons in the atom.

After the integration, we can get the velocity distribution for atoms up to $Z = 26$ [58]:

$$f_{1s}(k) = \frac{32}{\pi} \frac{\mu_{1s}^5 k^2}{(\mu_{1s}^2 + k^2)^4} , \tag{A.4}$$

$$f_{2s}(k) = \frac{32}{3\pi} \frac{\mu_{2s}^5 (3\mu_{2s}^2 k - k^3)^2}{(\mu_{2s}^2 + k^2)^6} , \tag{A.5}$$

$$f_{2p}(k) = \frac{512}{3\pi} \frac{\mu_{2p}^7 k^4}{(\mu_{2p}^2 + k^2)^6} , \tag{A.6}$$

$$f_{3s}(k) = \frac{1024}{5\pi} \frac{\mu_{3s}^7 (\mu_{3s}^3 k - \mu_{3s} k^3)^2}{(\mu_{3s}^2 + k^2)^8} , \tag{A.7}$$

$$f_{3p}(k) = \frac{1024}{45\pi} \frac{\mu_{3p}^7 (5\mu_{3p}^2 k^2 - k^4)^2}{(\mu_{3p}^2 + k^2)^8} , \tag{A.8}$$

$$f_{3d}(k) = \frac{4096}{5\pi} \frac{\mu_{3d}^9 k^6}{(\mu_{3d}^2 + k^2)^8} , \tag{A.9}$$

$$f_{4s}(k) = \frac{512}{35\pi} \frac{\mu_{4s}^9 (5\mu_{4s}^4 k - 10\mu_{4s}^2 k^3 + k^5)^2}{(\mu_{4s}^2 + k^2)^{10}} . \tag{A.10}$$

Note that we have checked the expressions in ref. [58] and corrected possible discrepancies as in our eqs. (A.5) and (A.10).

We take the ice molecule H_2O as an example. For oxygen, $\mu_{1s} = 7.6579$, $\mu_{2s} = 2.2458$ and $\mu_{2p} = 2.2266$ [90], and for hydrogen $\mu_{1s} = 1$. We weigh the distribution functions by

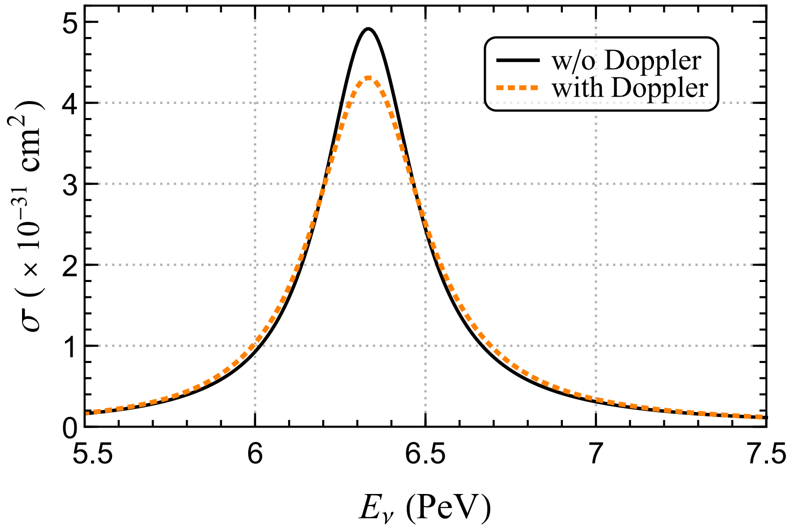

Figure 4. Cross section for the Glashow resonance process $\bar{\nu}_e + e^- \to W^- \to X$ with and without Doppler broadening and assuming ice (H_2O) as the target. The black curve represents the cross section without Doppler broadening and for the orange curve Doppler broadening is included.

averaging over the electron numbers:

$$F_{\text{ice}}(\beta) = \frac{2F_{\text{H}}(\beta) + 8F_{\text{O}}(\beta)}{10}\,. \tag{A.11}$$

Using eq. (A.1) together with eq. (A.11) we get the Doppler broadened cross section for ice as the target, which is depicted in figure 4. The effect reduces the peak by about 12%. Even though the total cross section integrated over the initial neutrino energy is barely altered, the broadening effect will make a difference when a non-uniform neutrino spectrum is considered.

Acknowledgments

GYH would like to thank Xiao-Jun Bi, Xun-Jie Xu, Shoushan Zhang and Shun Zhou for inspiring comments and discussions. GYH is supported in part by the Alexander von Humboldt Foundation.

References

[1] IceCube collaboration, *Detection of a particle shower at the Glashow resonance with IceCube*, *Nature* **591** (2021) 220 [*Erratum ibid.* **592** (2021) E11] [`arXiv:2110.15051`] [inSPIRE].

[2] IceCube collaboration, *Evidence for High-Energy Extraterrestrial Neutrinos at the IceCube Detector*, *Science* **342** (2013) 1242856 [`arXiv:1311.5238`] [inSPIRE].

[3] IceCube collaboration, *First observation of PeV-energy neutrinos with IceCube*, *Phys. Rev. Lett.* **111** (2013) 021103 [arXiv:1304.5356] [INSPIRE].

[4] IceCube collaboration, *Neutrino emission from the direction of the blazar TXS 0506+056 prior to the IceCube-170922A alert*, *Science* **361** (2018) 147 [arXiv:1807.08794] [INSPIRE].

[5] IceCube collaboration, *Detection of astrophysical tau neutrino candidates in IceCube*, *Eur. Phys. J. C* **82** (2022) 1031 [arXiv:2011.03561] [INSPIRE].

[6] IceCube collaboration, *The IceCube high-energy starting event sample: Description and flux characterization with 7.5 years of data*, *Phys. Rev. D* **104** (2021) 022002 [arXiv:2011.03545] [INSPIRE].

[7] IceCube collaboration, *Evidence for neutrino emission from the nearby active galaxy NGC 1068*, *Science* **378** (2022) 538 [arXiv:2211.09972] [INSPIRE].

[8] F. Halzen and A. Kheirandish, *IceCube and High-Energy Cosmic Neutrinos*, in *The Encyclopedia of Cosmology*, F.W. Stecker, World Scientific (2023), chapter 5, pp. 107–235 [DOI:10.1142/9789811282645_0005] [arXiv:2202.00694] [INSPIRE].

[9] T.K. Gaisser, F. Halzen and T. Stanev, *Particle astrophysics with high-energy neutrinos*, *Phys. Rep.* **258** (1995) 173 [hep-ph/9410384] [INSPIRE].

[10] P. Bhattacharjee and G. Sigl, *Origin and propagation of extremely high-energy cosmic rays*, *Phys. Rep.* **327** (2000) 109 [astro-ph/9811011] [INSPIRE].

[11] J.J. Beatty and S. Westerhoff, *The Highest-Energy Cosmic Rays*, *Ann. Rev. Nucl. Part. Sci.* **59** (2009) 319 [INSPIRE].

[12] T.K. Gaisser, R. Engel and E. Resconi, *Cosmic Rays and Particle Physics*, second edition, Cambridge University Press (2016) [DOI:10.1017/cbo9781139192194].

[13] L.A. Anchordoqui, *Ultra-High-Energy Cosmic Rays*, *Phys. Rep.* **801** (2019) 1 [arXiv:1807.09645] [INSPIRE].

[14] J.B. Tjus and L. Merten, *Closing in on the origin of Galactic cosmic rays using multimessenger information*, *Phys. Rep.* **872** (2020) 1 [arXiv:2002.00964] [INSPIRE].

[15] K. Murase and I. Bartos, *High-Energy Multimessenger Transient Astrophysics*, *Ann. Rev. Nucl. Part. Sci.* **69** (2019) 477 [arXiv:1907.12506] [INSPIRE].

[16] K. Murase and F.W. Stecker, *High-Energy Neutrinos from Active Galactic Nuclei*, in *The Encyclopedia of Cosmology*, F.W. Stecker ed., World Scientific (2023), chapter 10, pp. 483–540 [arXiv:2202.03381] [DOI:10.1142/9789811282645_0010] [INSPIRE].

[17] S.V. Troitsky, *Constraints on models of the origin of high-energy astrophysical neutrinos*, *Usp. Fiz. Nauk* **191** (2021) 1333 [arXiv:2112.09611] [INSPIRE].

[18] Z.-Z. Xing and S. Zhou, *Neutrinos in particle physics, astronomy and cosmology*, Zhejiang University Press (2011) [ISBN: 9783642175596, 9787308080248] [INSPIRE].

[19] O. Mena, S. Palomares-Ruiz and A.C. Vincent, *Flavor Composition of the High-Energy Neutrino Events in IceCube*, *Phys. Rev. Lett.* **113** (2014) 091103 [arXiv:1404.0017] [INSPIRE].

[20] C.-Y. Chen, P.S. Bhupal Dev and A. Soni, *Two-component flux explanation for the high energy neutrino events at IceCube*, *Phys. Rev. D* **92** (2015) 073001 [arXiv:1411.5658] [INSPIRE].

[21] S. Palomares-Ruiz, A.C. Vincent and O. Mena, *Spectral analysis of the high-energy IceCube neutrinos*, *Phys. Rev. D* **91** (2015) 103008 [`arXiv:1502.02649`] [INSPIRE].

[22] IceCube collaboration, *Flavor Ratio of Astrophysical Neutrinos above* 35 *TeV in IceCube*, *Phys. Rev. Lett.* **114** (2015) 171102 [`arXiv:1502.03376`] [INSPIRE].

[23] A. Palladino, G. Pagliaroli, F.L. Villante and F. Vissani, *What is the Flavor of the Cosmic Neutrinos Seen by IceCube?*, *Phys. Rev. Lett.* **114** (2015) 171101 [`arXiv:1502.02923`] [INSPIRE].

[24] C.A. Argüelles, T. Katori and J. Salvado, *New Physics in Astrophysical Neutrino Flavor*, *Phys. Rev. Lett.* **115** (2015) 161303 [`arXiv:1506.02043`] [INSPIRE].

[25] M. Bustamante, J.F. Beacom and W. Winter, *Theoretically palatable flavor combinations of astrophysical neutrinos*, *Phys. Rev. Lett.* **115** (2015) 161302 [`arXiv:1506.02645`] [INSPIRE].

[26] IceCube collaboration, *A combined maximum-likelihood analysis of the high-energy astrophysical neutrino flux measured with IceCube*, *Astrophys. J.* **809** (2015) 98 [`arXiv:1507.03991`] [INSPIRE].

[27] V. Brdar, J. Kopp and X.-P. Wang, *Sterile Neutrinos and Flavor Ratios in IceCube*, *JCAP* **01** (2017) 026 [`arXiv:1611.04598`] [INSPIRE].

[28] G. D'Amico, *Flavor and energy inference for the high-energy IceCube neutrinos*, *Astropart. Phys.* **101** (2018) 8 [`arXiv:1712.04979`] [INSPIRE].

[29] G. Pagliaroli, A. Palladino, F.L. Villante and F. Vissani, *Testing nonradiative neutrino decay scenarios with IceCube data*, *Phys. Rev. D* **92** (2015) 113008 [`arXiv:1506.02624`] [INSPIRE].

[30] R.W. Rasmussen, L. Lechner, M. Ackermann, M. Kowalski and W. Winter, *Astrophysical neutrinos flavored with Beyond the Standard Model physics*, *Phys. Rev. D* **96** (2017) 083018 [`arXiv:1707.07684`] [INSPIRE].

[31] V. Brdar and R.S.L. Hansen, *IceCube Flavor Ratios with Identified Astrophysical Sources: Towards Improving New Physics Testability*, *JCAP* **02** (2019) 023 [`arXiv:1812.05541`] [INSPIRE].

[32] M. Bustamante and M. Ahlers, *Inferring the flavor of high-energy astrophysical neutrinos at their sources*, *Phys. Rev. Lett.* **122** (2019) 241101 [`arXiv:1901.10087`] [INSPIRE].

[33] A. Palladino, *The flavor composition of astrophysical neutrinos after 8 years of IceCube: an indication of neutron decay scenario?*, *Eur. Phys. J. C* **79** (2019) 500 [`arXiv:1902.08630`] [INSPIRE].

[34] IceCube collaboration, *IceCube High Energy Starting Events at 7.5 Years — New Measurements of Flux and Flavor*, *EPJ Web Conf.* **207** (2019) 02005 [`arXiv:1905.04237`] [INSPIRE].

[35] N. Song, S.W. Li, C.A. Argüelles, M. Bustamante and A.C. Vincent, *The Future of High-Energy Astrophysical Neutrino Flavor Measurements*, *JCAP* **04** (2021) 054 [`arXiv:2012.12893`] [INSPIRE].

[36] S.L. Glashow, *Resonant Scattering of Antineutrinos*, *Phys. Rev.* **118** (1960) 316 [INSPIRE].

[37] V.S. Berezinsky and A.Z. Gazizov, *Cosmic neutrino and the possibility of Searching for W bosons with masses* 30–100 *GeV in underwater experiments*, *JETP Lett.* **25** (1977) 254 [INSPIRE].

[38] R.W. Brown and F.W. Stecker, *Cosmic Ray Neutrino Tests for Heavier Weak Bosons and Cosmic Antimatter*, *Phys. Rev. D* **26** (1982) 373 [INSPIRE].

[39] L.A. Anchordoqui, H. Goldberg, F. Halzen and T.J. Weiler, *Neutrinos as a diagnostic of high energy astrophysical processes*, *Phys. Lett. B* **621** (2005) 18 [`hep-ph/0410003`] [INSPIRE].

[40] S. Hümmer, M. Maltoni, W. Winter and C. Yaguna, *Energy dependent neutrino flavor ratios from cosmic accelerators on the Hillas plot*, *Astropart. Phys.* **34** (2010) 205 [`arXiv:1007.0006`] [INSPIRE].

[41] Z.-Z. Xing and S. Zhou, *The Glashow resonance as a discriminator of UHE cosmic neutrinos originating from p-gamma and p-p collisions*, *Phys. Rev. D* **84** (2011) 033006 [`arXiv:1105.4114`] [INSPIRE].

[42] A. Bhattacharya, R. Gandhi, W. Rodejohann and A. Watanabe, *The Glashow resonance at IceCube: signatures, event rates and pp vs. $p\gamma$ interactions*, *JCAP* **10** (2011) 017 [`arXiv:1108.3163`] [INSPIRE].

[43] A. Bhattacharya, R. Gandhi, W. Rodejohann and A. Watanabe, *On the interpretation of IceCube cascade events in terms of the Glashow resonance*, `arXiv:1209.2422` [INSPIRE].

[44] V. Barger, J. Learned and S. Pakvasa, *IceCube PeV Cascade Events Initiated by Electron-Antineutrinos at Glashow Resonance*, *Phys. Rev. D* **87** (2013) 037302 [`arXiv:1207.4571`] [INSPIRE].

[45] V. Barger, L. Fu, J.G. Learned, D. Marfatia, S. Pakvasa and T.J. Weiler, *Glashow resonance as a window into cosmic neutrino sources*, *Phys. Rev. D* **90** (2014) 121301 [`arXiv:1407.3255`] [INSPIRE].

[46] A. Palladino, G. Pagliaroli, F.L. Villante and F. Vissani, *Double pulses and cascades above 2 PeV in IceCube*, *Eur. Phys. J. C* **76** (2016) 52 [`arXiv:1510.05921`] [INSPIRE].

[47] I.M. Shoemaker and K. Murase, *Probing BSM Neutrino Physics with Flavor and Spectral Distortions: Prospects for Future High-Energy Neutrino Telescopes*, *Phys. Rev. D* **93** (2016) 085004 [`arXiv:1512.07228`] [INSPIRE].

[48] L.A. Anchordoqui, M.M. Block, L. Durand, P. Ha, J.F. Soriano and T.J. Weiler, *Evidence for a break in the spectrum of astrophysical neutrinos*, *Phys. Rev. D* **95** (2017) 083009 [`arXiv:1611.07905`] [INSPIRE].

[49] M.D. Kistler and R. Laha, *Multi-PeV Signals from a New Astrophysical Neutrino Flux Beyond the Glashow Resonance*, *Phys. Rev. Lett.* **120** (2018) 241105 [`arXiv:1605.08781`] [INSPIRE].

[50] D. Biehl, A. Fedynitch, A. Palladino, T.J. Weiler and W. Winter, *Astrophysical Neutrino Production Diagnostics with the Glashow Resonance*, *JCAP* **01** (2017) 033 [`arXiv:1611.07983`] [INSPIRE].

[51] S. Sahu and B. Zhang, *On the non-detection of Glashow resonance in IceCube*, *J. High Energy Astrophys.* **18** (2018) 1 [`arXiv:1612.09043`] [INSPIRE].

[52] G.-Y. Huang and Q. Liu, *Hunting the Glashow Resonance with PeV Neutrino Telescopes*, *JCAP* **03** (2020) 005 [`arXiv:1912.02976`] [INSPIRE].

[53] S. Zhou, *Cosmic Flavor Hexagon for Ultrahigh-energy Neutrinos and Antineutrinos at Neutrino Telescopes*, `arXiv:2006.06181` [INSPIRE].

[54] IceCube collaboration, *The IceCube Neutrino Observatory — Contributions to ICRC 2015. Part II. Atmospheric and Astrophysical Diffuse Neutrino Searches of All Flavors*, in proceedings of the *34th International Cosmic Ray Conference (ICRC 2015)*, The Hague, The Netherlands, 30 July–6 August 2015, `arXiv:1510.05223` [inSPIRE].

[55] R. Gauld, *Precise predictions for multi-TeV and PeV energy neutrino scattering rates*, *Phys. Rev. D* **100** (2019) 091301 [`arXiv:1905.03792`] [inSPIRE].

[56] A. Garcia, R. Gauld, A. Heijboer and J. Rojo, *Complete predictions for high-energy neutrino propagation in matter*, *JCAP* **09** (2020) 025 [`arXiv:2004.04756`] [inSPIRE].

[57] I. Alikhanov, *On parton distributions in a photon gas*, *Eur. Phys. J. C* **65** (2010) 269 [`arXiv:0812.0937`] [inSPIRE].

[58] A. Loewy, S. Nussinov and S.L. Glashow, *The Effect of Doppler Broadening on the* 6.3 *PeV* W^- *Resonance in* $\bar{\nu}_e e^-$ *Collisions*, `arXiv:1407.4415` [inSPIRE].

[59] ALEPH et al. collaborations, *Precision electroweak measurements on the Z resonance*, *Phys. Rep.* **427** (2006) 257 [`hep-ex/0509008`] [inSPIRE].

[60] M. Cacciari, A. Deandrea, G. Montagna and O. Nicrosini, *QED structure functions: A Systematic approach*, *Europhys. Lett.* **17** (1992) 123 [inSPIRE].

[61] IceCube collaboration, *Observation of High-Energy Astrophysical Neutrinos in Three Years of IceCube Data*, *Phys. Rev. Lett.* **113** (2014) 101101 [`arXiv:1405.5303`] [inSPIRE].

[62] A.M. Hillas, *The Origin of Ultrahigh-Energy Cosmic Rays*, *Ann. Rev. Astron. Astrophys.* **22** (1984) 425 [inSPIRE].

[63] G. Cowan, *Statistical data analysis*, Clarendon Press (1998) [ISBN: 9780198501565].

[64] P. Baerwald, S. Hümmer and W. Winter, *Magnetic Field and Flavor Effects on the Gamma-Ray Burst Neutrino Flux*, *Phys. Rev. D* **83** (2011) 067303 [`arXiv:1009.4010`] [inSPIRE].

[65] S. Hümmer, M. Rüger, F. Spanier and W. Winter, *Simplified models for photohadronic interactions in cosmic accelerators*, *Astrophys. J.* **721** (2010) 630 [`arXiv:1002.1310`] [inSPIRE].

[66] IceCube collaboration, *IceCube-Gen2: A Vision for the Future of Neutrino Astronomy in Antarctica*, `arXiv:1412.5106` [inSPIRE].

[67] IceCube-Gen2 collaboration, *IceCube-Gen2: the window to the extreme Universe*, *J. Phys. G* **48** (2021) 060501 [`arXiv:2008.04323`] [inSPIRE].

[68] Baikal-GVD collaboration, *Baikal-GVD: status and prospects*, *EPJ Web Conf.* **191** (2018) 01006 [`arXiv:1808.10353`] [inSPIRE].

[69] KM3NeT collaboration, *Letter of intent for KM3NeT 2.0*, *J. Phys. G* **43** (2016) 084001 [`arXiv:1601.07459`] [inSPIRE].

[70] P-ONE collaboration, *The Pacific Ocean Neutrino Experiment*, *Nat. Astron.* **4** (2020) 913 [`arXiv:2005.09493`] [inSPIRE].

[71] A. Romero-Wolf et al., *An Andean Deep-Valley Detector for High-Energy Tau Neutrinos*, in proceedings of the *Latin American Strategy Forum for Research Infrastructure*, São Paulo, Brazil, 30 April–1 May 2019, `arXiv:2002.06475` [inSPIRE].

[72] Z.P. Ye et al., *Proposal for a neutrino telescope in South China Sea*, `arXiv:2207.04519` [inSPIRE].

JHEP11(2023)164

[73] G.-Y. Huang, S. Jana, M. Lindner and W. Rodejohann, *Probing new physics at future tau neutrino telescopes*, *JCAP* **02** (2022) 038 [arXiv:2112.09476] [INSPIRE].

[74] A. Coleman et al., *Ultra high energy cosmic rays The intersection of the Cosmic and Energy Frontiers*, *Astropart. Phys.* **147** (2023) 102794 [*Corrigendum ibid.* **149** (2023) 102819] [arXiv:2205.05845] [INSPIRE].

[75] M. Ackermann et al., *High-energy and ultra-high-energy neutrinos: A Snowmass white paper*, *J. High Energy Astrophys.* **36** (2022) 55 [arXiv:2203.08096] [INSPIRE].

[76] V.B. Valera, M. Bustamante and C. Glaser, *Near-future discovery of the diffuse flux of ultrahigh-energy cosmic neutrinos*, *Phys. Rev. D* **107** (2023) 043019 [arXiv:2210.03756] [INSPIRE].

[77] LHAASO collaboration, *Peta-electron volt gamma-ray emission from the Crab Nebula*, *Science* **373** (2021) 425 [arXiv:2111.06545] [INSPIRE].

[78] LHAASO collaboration, *Ultrahigh-energy photons up to* 1.4 *petaelectronvolts from* 12 *γ-ray Galactic sources*, *Nature* **594** (2021) 33 [INSPIRE].

[79] T. Sudoh and J.F. Beacom, *Where are Milky Way's hadronic PeVatrons?*, *Phys. Rev. D* **107** (2023) 043002 [arXiv:2209.03970] [INSPIRE].

[80] M. Bustamante, *New limits on neutrino decay from the Glashow resonance of high-energy cosmic neutrinos*, arXiv:2004.06844 [INSPIRE].

[81] T. Ježo, M. Klasen, F. Lyonnet, F. Montanet, I. Schienbein and M. Tartare, *Can new heavy gauge bosons be observed in ultra-high energy cosmic neutrino events?*, *Phys. Rev. D* **89** (2014) 077702 [arXiv:1401.6012] [INSPIRE].

[82] K.S. Babu, P.S. Dev, S. Jana and Y. Sui, *Zee-Burst: A New Probe of Neutrino Nonstandard Interactions at IceCube*, *Phys. Rev. Lett.* **124** (2020) 041805 [arXiv:1908.02779] [INSPIRE].

[83] U.K. Dey, N. Nath and S. Sadhukhan, *Charged Higgs effects in IceCube: PeV events and NSIs*, *JHEP* **09** (2021) 113 [arXiv:2010.05797] [INSPIRE].

[84] K.S. Babu, P.S.B. Dev and S. Jana, *Probing neutrino mass models through resonances at neutrino telescopes*, *Int. J. Mod. Phys. A* **37** (2022) 2230003 [arXiv:2202.06975] [INSPIRE].

[85] D.-H. Xu and S.-J. Rong, *Connect the Lorentz violation to the Glashow resonance event*, *Mod. Phys. Lett. A* **38** (2023) 2350029 [arXiv:2211.05478] [INSPIRE].

[86] C.A. Argüelles et al., *Snowmass white paper: beyond the standard model effects on neutrino flavor*, in proceedings of the *Snowmass 2021*, Seattle, WA, U.S.A., 17–26 July 2022, *Eur. Phys. J. C* **83** (2023) 15 [arXiv:2203.10811] [INSPIRE].

[87] G.-Y. Huang, S. Jana, M. Lindner and W. Rodejohann, *Probing heavy sterile neutrinos at neutrino telescopes via the dipole portal*, *Phys. Lett. B* **840** (2023) 137842 [arXiv:2204.10347] [INSPIRE].

[88] G.-Y. Huang, *Double and multiple bangs at tau neutrino telescopes*, *Eur. Phys. J. C* **82** (2022) 1089 [arXiv:2207.02222] [INSPIRE].

[89] R. Heighton, L. Heurtier and M. Spannowsky, *Hunting for neutral leptons with ultrahigh-energy neutrinos*, *Phys. Rev. D* **108** (2023) 055009 [arXiv:2303.11352] [INSPIRE].

[90] E. Clementi and D.L. Raimondi, *Atomic Screening Constants from SCF Functions*, *J. Chem. Phys.* **38** (1963) 2686.